Journal of Engineering Research and Reports

17(2): 34-50, 2020; Article no.JERR.61548
ISSN: 2582-2926

Analysis of Ethylene Glycol (EG)-based ((Cu-Al_2O_3), (Cu-TiO_2), (TiO_2-Al_2O_3)) Hybrid Nanofluids for Optimal Car Radiator Coolant

J. A. Okello[1*], W. N. Mutuku[1] and A. O. Oyem[2]

[1]Department of Mathematics and Actuarial Science, Kenyatta University, Kenya.
[2]Department of Mathematics and Statistics, Islamic University, Uganda.

Authors' contributions

This work was carried out in collaboration among all authors. All authors jointly designed the study and wrote the first draft of the manuscript. All authors did the simulations independently and their results agreed. All authors read and approved the final manuscript.

Article Information

DOI: 10.9734/JERR/2020/v17i217186
Editor(s):
(1) Dr. Guang Yih Sheu, Chang-Jung Christian University, Taiwan.
Reviewers:
(1) M. Anish, Sathyabama Institute of Science and Technology, India.
(2) Davood Toghraie, Islamic Azad University, Iran.
Complete Peer review History: http://www.sdiarticle4.com/review-history/61548

Original Research Article

Received 15 July 2020
Accepted 22 September 2020
Published 07 October 2020

ABSTRACT

Coolants are vital in any automotive since they manage the heat in the internal combustion of the engines by preventing corrosion in the cooling system as well as assist in eradicating the engine's waste heat. This paper examines three different types of ethylene glycol-based hybrid nanofluids ((Cu-Al_2O_3), (Cu-TiO_2), (TiO_2-Al_2O_3)) to establish their cooling capabilities for industrial cooling applications. The vertical flow of these hybrid nanofluids combination through a semi-infinite convectively heated flat plate mimicking the flow of coolant in car radiator is modeled. The governing non-linear partial differential equations of fluid flow are transformed into a system of coupled non-linear ordinary differential equations using a suitable similarity transformation variables and the numerical solution executed using the shooting technique together with the fourth-order Runge-Kutta-Fehlberg integration scheme. The numerical simulation is executed using MATLAB and results are displayed graphically. The effects of pertinent parameters on velocity, temperature, skin friction, and local Nusselt number are investigated. From the study (Cu-Al_2O_3)/ EG hybrid nanocoolant leads to a rapid decrease in temperature at the boundary layer.

Keywords: Hybrid nanofluids; industrial hybrid nanocoolants; radiator.

**Corresponding author: Email: acholajohn2010@gmail.com;*

NOMENCLATURES

(u, v)	*Velocity components*
ρ	*Density*
(x, y)	*Coordinates*
ψ	*Stream function*
T	*Temperature*
σ	*Electrical conductivity*
T_∞	*Free stream temperature*
μ	*Dynamic viscosity*
B_0	*Constant applied magnetic field*
U_∞	*Free stream velocity*
β	*Thermal expansion coefficient*
ϕ	*Nanoparticle concentration*
Bi	*Local Biot number*
Pr	*Prandtl number*
Gr	*Grashof number*
Ec	*Eckert number*
Ha	*Magnetic field intensity parameter*
Nu_X	*Local Nusselt number*
θ	*Dimensionless temperature*
η	*Transverse distance*

SUBSCRIPT

hnf –Hybrid Nanofluid

1. INTRODUCTION

Thermal management of industrial waste heat and heat dissipated by engineering equipment is important for operational efficiency and the overall life span of the equipment. The use of conventional heat transfer fluids (such as water, ethylene glycol, and engine oil) as coolants in heat exchangers is limited by their inherent poor thermal transfer properties. Choi [1] proposed addition of nanoparticles in the conventional heat transfer fluids to enhance their thermal conductivity. The resulting fluids dispersed with nanoparticles were called nanofluids. Nanofluids are synthesized by suspending nanosized particles in the base fluid. The nanoparticles commonly used are made of metals (Cu, Ag, Ni, and Au), metal oxides (Al_2O_3, CuO, MgO, ZnO, SiO_2, Fe_2O_3, and TiO_2), metal carbide (SiC), metal nitride (AIN), or Carbon materials (CNTs, MWCNTs, diamond, and graphite) and the base fluid consist of conventional heat transfer fluids such as water, ethylene glycol, engine oil, transformer oil, vegetable oil, kerosene, toluene, etc.

Nanofluids are used in an array of heat transfer applications such as automotive, Biomedical, Electronic, space and Defense, Geothermal, Solar energy, and nuclear energy fields owing to their advanced thermophysical properties (thermal conductivity, thermal diffusivity, viscosity, and convective heat transfer coefficient).

Thermal conductivity and viscosity are crucial in heat transfer applications of the nanofluid. The thermal conductivity enhancement leads to higher heat transfer rate and thermal efficiency while the viscosity of the nanofluid influences both convective heat transfer, pressure drop, and pumping power requirement [2] . A study by Yan et al. [3] on the rheological behavior of MWCNTs-ZnO / Water-Ethylene glycol $(80:20\ vol.\%)$ hybrid nanofluid observed enhancement in viscosity by more than 90% at a temperature of $25℃$ by increasing φ from $(0-1.2\%)$. They also reported reduction in viscosity by 21%, 17%, and 8% for a temperature of $T = 50℃, 40℃$ and $30℃$ at $\varphi = 1.2\%$ with reference to a temperature of $25℃$. Boroomandpour et al. [4] in their study on thermal conductivity of a ternary hybrid nanofluid containing MWCNTs-Titania-Zinc oxide / water-ethylene glycol $(80:20)$ reported maximum enhancement in thermal conductivity by 17.82% compared to base fluid for MWCNTs / water-ethylene glycol nanofluid at $\varphi = 0.4\%$ and $T = 50℃$. Madhesh et al. [5] investigating heat transfer characteristic of (Cu-Ti /H_2O) hybrid nanofluid for possible application as a coolant fluid reported improved convective heat transfer coefficient of up to 48.4% at 0.7% nanoparticle volume concentration. Mosayebidorcheh et al. [6] observed linear increase in convective heat transfer coefficient with increasing nanoparticle volume concentration and Reynolds number. A study by Hassan et al. [7] into convective heat transfer and flow characteristics of (Cu-Ag/H_2O) hybrid nanofluid revealed enhanced heat transfer coefficient of the hybrid nanofluid compared to the base fluid and mono (single material) nanofluids of (Cu/H_2O and Ag/H_2O). Tayebi & Chamkha [8] reported better enhancement in heat transfer rate in (Cu-Al_2O_3/H_2O) hybrid nanofluid compared to a single material (Al_2O_3/H_2O) nanofluid. Soltani et al. [9] investigating thermal conductivity of (WO_3-MWCNTs)/ Engine oil hybrid nanofluid noted enhancement in thermal conductivity with increasing temperature and volume fraction of the nanoparticles. The maximum thermal conductivity enhancement of 19.85% compared to the base fluid was recorded at a temperature of $60℃$ and nanoparticle volume fraction of $\varphi = 0.6\%$. Alrashed et al. [10] researching on convection of H_2O/MWCNT through a backward-

facing contracting channel, they observed a reduction in surface temperature and enhancement in heat transfer coefficient with increasing Reynolds number or weight percentage of nanoparticles in water/FMWCNT nanofluid.

Nagarajan et al. [11] investigating the heat transfer intensification rate using (alumina-silica)/Ethylene glycol nanocoolant revealed an increment in heat transfer coefficient of nanofluid by 52.8% compared to 50% of pure ethylene glycol. Selvaraj & Krishnan [12] using graphene encased alumina as a coolant fluid in electronic devices reported enhancement in thermal conductivity of the nanofluid by a maximum value of $(45\%\pm3\%)$ at (0-0.3vol%) particle loading and temperature range of $(20-70℃)$ compared to base fluid-DI water. The heat transfer coefficient was enhanced by $51.73\%(\pm2\%)$ at (150-650) Reynolds number and (0-0.2vol %) nanofluid concentration. Deriszadeh & Monte [13] using (Al_2O_3/H_2O) nanofluid in electric motor cooling system observed enhancement in heat transfer coefficient by 25% and 32% at 2% and 4% nanoparticle volume fraction respectively. The electric motor operating temperature decreased with an increase in the Reynolds number. The experiment conducted by Pourrajab et al. [14] on (Cu/SBA-15) water-based hybrid nanofluid in weight fractions of (0.019-0.075%) and temperature range of $(25-50℃)$ revealed an increase in thermal conductivity of the hybrid nanofluid by 24.24% with increasing nanocomposite concentration and temperature. They concluded that the hybrid nanofluid could be applied as a heat transfer fluid in thermal engineering systems.

Mukherjee et al. [15] experimenting with (Al_2O_3/H_2O) and (TiO_2/H_2O) nanofluids reported enhanced thermal conductivity and heat transfer by both nanofluids compared to the use of base fluid (water) alone. The (Al_2O_3-water) nanofluids registered better thermal conductivity and heat transfer compared to TiO_2/H_2O nanofluids with maximum enhancement in thermal conductivity and heat transfer of Al_2O_3-water nanofluids being 44% and 21% respectively. A study by Kumar & Chandrasekar [16] to determine heat transfer and friction factor of MWCNT nanofluid in double helically coiled tube heat exchanger reported higher convective heat transfer in (MWCNT/water) based nanofluid compared to water alone. The highest convective heat transfer obtained using MWCNT/H_2O nanofluid was 35% at 0.6% nanoparticle volume concentration. Pourrajab, Noghrehabadi, Behbahani, et al. [17] using (MWCNTs-COOH/Ag)-water based hybrid nanofluid reported increment in thermal conductivity by 47.3% above that of the base fluid for 0.04vol% (Ag)-0.16vol% MWCNTs hybrid nanofluid.

The behavior of nanofluid (heat transfer and pressure drop) in the heat exchanger (radiator) that serves as a heat sink in automobiles engines, piston engines of aircraft, locomotives (trains), and motorcycles is important in cooling applications of the nanofluid in the radiator. The incorporation of nanofluid in the radiator fast-tracks the removal of heat from the engine block system by the circulating nanofluid. Studies by [18-19] revealed that incorporating nanofluid in radiators leads to smaller sized radiators with enhanced cooling capability, possible reduction in the frontal area of the automobiles resulting in improved aerodynamic design for fuel efficiency since smaller sized radiators allows for better positioning of the radiator which improves the aerodynamic design reducing drag from oncoming wind. M'hamed et al. [20] using MWCT nanocoolant in volume concentrations of (0.1%, 0.25%, 0.50%) dispersed in (50:50 H_2O/EG) mixture in *Perodua Kelisa 1000cc radiator system* reported enhancement in heat transfer coefficient with increasing volume concentration and Reynolds number. The maximum average heat transfer coefficient enhancement registered was 196.3% at 0.5% nanoparticle volume concentration. Mutuku [21] investigating ethylene-glycol based nanofluids (CuO, Al_2O_3, TiO_2) as a coolant fluid in automotive radiator reported a rapid decrease in temperature in CuO-EG based nanofluid compared to the rest of nanofluids. Huminic & Huminic [22] using (MWCNT-Fe_3O_4/water) hybrid nanofluid as a coolant fluid for automotive applications reported enhancement in heat transfer with increasing volume concentration of hybrid nanoparticles and increasing Reynolds number. The range of Reynolds number was (50-1000) and the volume concentration of nanoparticles used was 0.1% and 0.3%. Barzegarian et al. [23] studying water-based Al_2O_3-gamma nanofluid in shell and tube heat exchanger radiator at 0.3vol. % concentration reported enhancement of 29.8% in Nusselt number and 19.1% in heat transfer coefficient compared to base fluid alone. Hussein [24] utilizing (Aluminum Nitride/EG) nanofluid in double pipe heat exchanger at 4% volume concentration reported improvement in thermal performance by 35% above that of the base fluid.

Raei et al. [25] using (gamma-Al_2O_3/H_2O)-nanofluid in double tube heat exchanger at 0.15vol. % concentration and nanoparticle size of 20nm reported enhancement in heat transfer coefficient by 25% compared to use of water alone. Study by Hung et al. [26] on hybrid nanofluid air-cooled heat exchange system using hybrid carbon (20-30nm)/H_2O nanofluid at 0.02wt. % concentration recorded enhancement in heat exchange capacity by 13% and improvement in system efficiency factor by 11.7%.

The conductive nature of nanofluids makes them more susceptible to the effects of magnetic fields compared to conventional fluids [27]. The problems of (MHD) flows are common in engineering and industrial processes. They are applicable in areas such as purification of crude oil, textile industry, polymer technology, metallurgy, extrusion of plastic in the manufacture of Rayon and Nylon, and cooling of reactors.

The previous research conducted on the use of nanofluid as a coolant fluid in car radiator concentrated on nanofluids containing a single type nanoparticle (mono nanofluids) with water as the base fluid. The current paper explores the use of hybrid nanofluid as a coolant fluid in a car radiator with ethylene-glycol as the base fluid. The paper extends Mutuku [21] work by incorporating hybrid nanofluid in the flow. The vertical flow of hybrid nanofluid through a semi-infinite convectively heated flat plate representing the flow of coolant in the car radiator is considered. The governing non-linear partial differential equations representing the flow are transformed into a system of coupled non-linear ordinary differential equations using a suitable similarity transformation variables and the numerical solution arrived at using the shooting technique together with the fourth-order Runge-Kutta-Fehlberg integration scheme. The numerical simulation is then executed using MATLAB and the results displayed graphically.

2. MATHEMATICAL FORMULATION

A steady two-dimensional incompressible laminar boundary layer flow of an electrically conducting hybrid nanofluid past a convectively heated vertical semi-infinite flat plate under the influence of a transversely imposed magnetic field is considered. The left side of the plate is heated convectively by a hot fluid at a temperature T_f with a heat transfer coefficient h_f. A constant magnetic field of strength B_0 is imposed perpendicular to the flow. There is no applied voltage and the magnetic Reynolds number is small, hence the induced magnetic field and Hall effects are negligible (see Fig. 2).

The equations governing the two dimensional incompressible steady laminar flow illustrated in Fig. 1 are:

$$\frac{\partial u}{\partial x} + \frac{\partial v}{\partial y} = 0 \tag{1}$$

$$u\frac{\partial u}{\partial x} + v\frac{\partial u}{\partial y} = \frac{\mu_{hnf}}{\rho_{hnf}}\frac{\partial^2 u}{\partial y^2} + \beta_{hnf} g(T - T_\infty) - \frac{\sigma_{hnf}\beta_0^2 u}{\rho_{hnf}} \tag{2}$$

$$u\frac{\partial T}{\partial x} + v\frac{\partial T}{\partial y} = \frac{k_{hnf}}{(\rho C_p)_{hnf}}\frac{\partial^2 T}{\partial y^2} + \frac{\mu_{hnf}}{(\rho C_p)_{hnf}}\left(\frac{\partial u}{\partial y}\right)^2 + \frac{\sigma_{hnf}B_0^2 u^2}{(\rho C_p)_{hnf}} \tag{3}$$

The boundary conditions are:

$$\begin{aligned} &at\ y = 0: \quad u(x,0) = U_0, \quad v(x,0) = 0, \quad -k_f\frac{\partial T}{\partial y}(x,0) = h_f\left(T_f - T(x,0)\right) \\ &as\ y \to \infty: \ u(x,\infty) = 0,\ T(x,\infty) = T_\infty \end{aligned} \tag{4}$$

The equations $(1-3)$ plus the boundary conditions (4) is the extension of Mutuku [21] work when we incorporate hybrid nanofluid flow. Here $(\rho C_p)_{hnf}$ denotes heat capacitance of the hybrid nanofluid, $(u, v,)$ velocity component of the fluid in $(x, y,)$ directions, T is the local temperature of the fluid, k_{hnf} thermal conductivity of the hybrid nanofluid, ρ_{hnf} density of the hybrid nanofluid, μ_{hnf} is the dynamic viscosity of the hybrid nanofluid, g gravitational force, β_{hnf} the thermal expansion coefficient of the hybrid nanofluid, ϕ is the nanoparticle concentration and B_0 the constant magnetic field. The thermophysical properties of hybrid nanofluids are stated as follows:

$$\rho_{hnf} = \{(1-\phi_2)[(1-\phi_1)\rho_f + \phi_1\rho s_1]\} + \phi_2\rho s_2 \tag{5a}$$

$$\mu_{hnf} = \frac{\mu_f}{(1-\phi_1)^{2.5}(1-\phi_2)^{2.5}} \tag{5b}$$

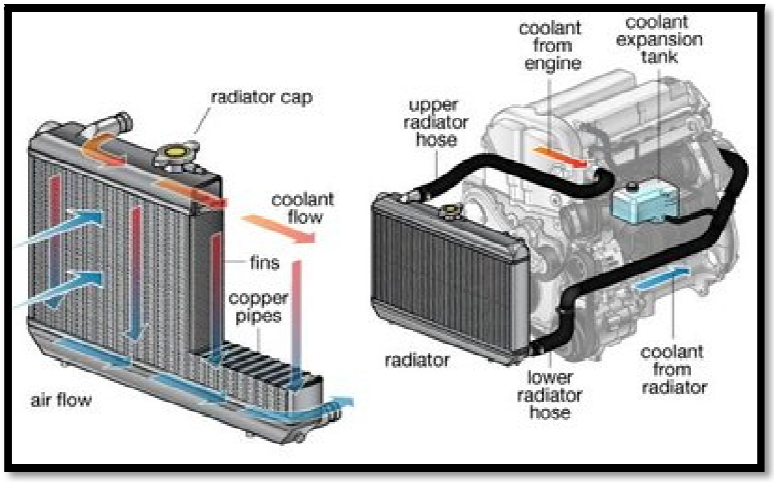

Fig. 1. The car radiator cooling system
(Michael & Company.com website)

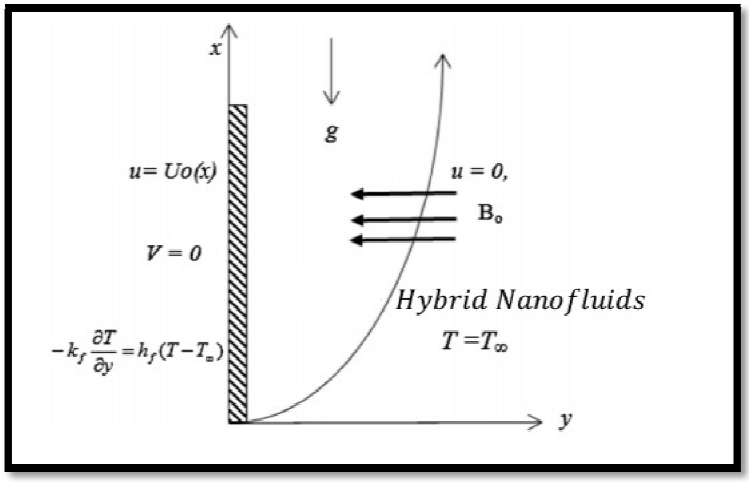

Fig. 2. Schematic diagram of hybrid nanofluid flow

$$\rho C_{p_{hnf}} = \left\{(1-\phi_2)\left[(1-\phi_1)(\rho C_p)_f + \phi 1\rho Cps1 + \phi 2\rho Cps2\right.\right. \quad (5c)$$

$$\beta_{hnf} = (1-\phi_1)(1-\phi_2)\beta_f + \phi_1\beta_{s_1} + \phi_2\beta_{s_2} \quad (5d)$$

$$k_{hnf} = \frac{k_{s_2} + (n-1)k_{bf} - (n-1)\phi_2(k_{bf} - k_{s_2})}{k_{s_2} + (n-1)k_{bf} + \phi_2(k_{bf} - k_{s_2})}(k_{bf}) \quad (5e)$$

To introduce the stream function $\psi(x,y)$ in the flow we define u and v as shown in equation (6) below:

$$u = \frac{\partial\psi}{\partial y}, \qquad v = -\frac{\partial\psi}{\partial x} \quad (6)$$

Using equation (6), the equation of continuity (1) is satisfied automatically as shown in equation (7):

$$\frac{\partial}{\partial x}\left(\frac{\partial\psi}{\partial y}\right) + \frac{\partial}{\partial y}\left(-\frac{\partial\psi}{\partial x}\right) = \frac{\partial^2\psi}{\partial x\partial y} - \frac{\partial^2\psi}{\partial x\partial y} = 0 \quad (7)$$

Introducing dimensionless quantities (8) in the flow and using them to solve equations (2) and (3) yields equations (9) and (10)

$$\eta = \left(a/v_f\right)^{1/2} y, \qquad \psi = \left(av_f\right)^{1/2} xf(\eta) \qquad \theta(\eta) = \frac{T-T_\infty}{T_W-T_\infty} \quad (8)$$

$$\frac{\mu_{hnf}}{\rho_{hnf}v_f} f''' + Gr\theta - Haf' - \left(f'\right)^2 + ff'' = 0 \quad (9)$$

$$\frac{\alpha_{hnf}}{\alpha_{bf}}\theta'' + PrEc\left(f''\right)^2 + PrEcHa\left(f'\right)^2 + Prf\theta' = 0 \quad (10)$$

Where the quantities; Ha-Hartman number, Gr-Grashof number, Pr-Prandtl number and Ec-Eckert number are defined as:

$$Ha = \frac{\sigma_{hnf}B_0^2}{a\rho_{hnf}},\ Gr = \frac{\beta_{hnf}g(T_W - T_\infty)}{a^2x},\ Pr = \frac{\nu_f}{\propto_{bf}},\ Ec = \frac{a^2x^2}{(C_p)_{hnf}(T_W - T_\infty)} \quad (11)$$

The set of boundary conditions for equations (9) and (10) are given by equations (12) as:

$$f(0) = 0,\quad f'(0) = 1,\quad \theta'(0) = Bi[\theta(0) - 1],\quad f'(\infty) = 0,\quad \theta(\infty) = 0 \quad (12)$$

For engineering and industrial application purposes, the physical quantities of practical significance are the skin friction coefficient C_f and the Nusselt number Nu defined as:

$$C_f = \frac{\tau_w}{\rho_f U_0^2},\qquad Nu = \frac{xq_w}{k_f(T_f - T_\infty)}, \quad (13)$$

Where τ_w is the skin friction and q_w is the surface heat flux given by

$$\tau_w = \mu_{hnf}\left.\frac{\partial u}{\partial y}\right|_{y=0},\ \ q_w = -k_{hnf}\left.\frac{\partial T}{\partial y}\right|_{y=0} \quad (14)$$

Putting equations (14) into (13) and simplifying yields:

$$C_{f_x} = Re_x^{1/2}C_f = \frac{1}{(1-\phi_1)^{2.5}(1-\phi_2)^{2.5}}f''(0) \quad (15)$$

$$Nu_x = Re_x^{-1/2}Nu = -\frac{k_{hnf}}{k_f}\theta'(0) \quad (16)$$

Where C_{f_x} and Nu_x are local skin friction and local Nusselt number respectively and $Re = \frac{U_0 x}{\nu_f}$ is the local Reynolds number.

2.1 Numerical Procedure

The coupled nonlinear boundary value problems given by equations (9) and (10) subject to the boundary conditions (12) are numerically solved using the shooting technique together with the fourth-order Runge-Kutta-Fehlberg iteration scheme. The equations are transformed into a set of initial value problems (IVPs) with unknown initial values that are determined by guessing, after which the fourth-order Runge-Kutta-Fehlberg iteration scheme is employed in integrating the set of IVPs until the given boundary conditions are satisfied.

The new variables are defined as follows:

$$x_1 = f,\quad x_2 = f',\quad x_3 = f'',\quad x_4 = \theta,\quad x_5 = \theta' \quad (17)$$

Using the new variables defined in equation (17), the equations (9) and (10) are transformed into a system of first-order differential equations (18) and (19) below:

$$\frac{\mu_{hnf}}{\rho_{hnf}\nu_f}x_3' = -Grx_4 + Hax_2 + x_2^2 - x_1x_3 \quad (18)$$

$$\frac{\propto_{hnf}}{\propto_{bf}}x_5' = -PrEcx_3^2 - PrEcHax_2^2 - Prx_1x_5 \quad (19)$$

The equations (18) and (19) are subject to the initial conditions:

$$x_1(0) = 0,\quad x_2(0) = 1,\quad x_5(0) = Bi[x_4(0) - 1]$$

$$x_2(0) = s_1,\qquad x_5(0) = s_2 \quad (20)$$

3. RESULTS AND DISCUSSION

The three different types of hybrid nanoparticle combination considered for hybrid nanocoolant are (Cu-Al_2O_3), (Cu-TiO_2) and (TiO_2-Al_2O_3). The hybrid nanoparticle combinations are then suspended in Ethylene-glycol base fluid. The graphical illustration of the results is given in Figs. $(3-23)$. The conclusion drawn from the flow is important in determining optimal hybrid nanoparticle combination for hybrid nanocoolant for industrial and engineering applications. $Ha = 0$ denotes the absence of the magnetic field and $\phi_1 = \phi_2 = 0$ represents regular fluid. The thermophysical properties of ethylene-glycol and nanoparticles are given in Table 1.

3.1 Dimensionless Velocity and Temperature Profiles of (Cu-Al_2O_3), (Cu-TiO_2) and (TiO_2-Al_2O_3) Ethylene-Glycol Based Hybrid Nanocoolants

Figs. 3 and 4 give primary velocity profiles and temperature profiles of ethylene-glycol based ((Cu-Al_2O_3), (Cu-TiO_2), and (TiO_2-Al_2O_3)) hybrid nanocoolants. From Fig. 3 the momentum boundary thickness of (TiO_2-Al_2O_3)/EG hybrid nanocoolant is thinner compared to the rest of hybrid nanocoolants which is attributed to the

fact that (TiO_2-Al_2O_3) hybrid nanoparticles combination is more susceptible to the influence of magnetic field compared to the rest of hybrid nanoparticle combinations. In Fig. 4 for both of the hybrid nanocoolants, the temperature is highest close to the surface of the plate and decays to zero value far away from the surface of the plate satisfying the given free stream condition. For the three given hybrid nanocoolants (Cu-Al_2O_3)/EG hybrid nanocoolant registered greater thermal boundary layer thickness compared to the rest of the nanocoolants.

3.2 Dimensionless Velocity and Temperature Profiles of (Cu-Al_2O_3)/Ethylene Glycol-Based Hybrid Nanocoolant

Figs. 5 and 6 illustrate the effect of increasing magnetic field intensity (Ha) on primary and secondary velocity profiles of (Cu-Al_2O)/Ethylene glycol-based hybrid nanocoolant. From Figs. 5 and 6 both the Primary velocity and secondary velocity of hybrid nanocoolant decreases with increasing values of Ha. The presence of Magnetic field in the flow results in the creation of Lorentz force in the flow ($\boldsymbol{F} = \boldsymbol{j} \times \boldsymbol{B}$) attributed to the motion of conducting fluid in the presence of a magnetic field that results in resistance or retardation of the flow of the fluid.

Figs 7, 8, and 9 illustrate the effect of nanoparticle volume fraction and Eckert number on primary and secondary velocity profiles of (Cu-Al_2O_3)/EG hybrid nanocoolant. From Fig. 7 the primary velocity profiles of the nanocoolant increases with the increasing nanoparticle volume fraction (ϕ). In both Figs. 8 and 9 both the primary velocity profiles and secondary velocity profiles of the (Cu-Al_2O_3)/EG hybrid nanocoolant increases with increasing Eckert number.

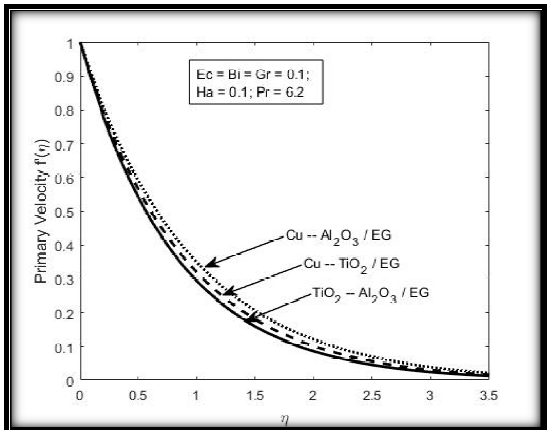

Fig. 3. Primary velocity profiles for different hybrid nanocoolants

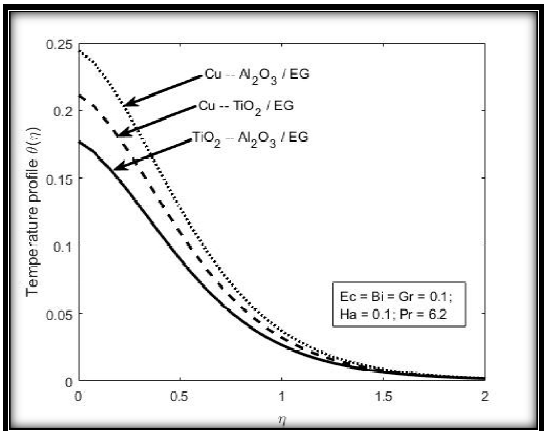

Fig. 4. Temperature profiles for different hybrid nanocoolants

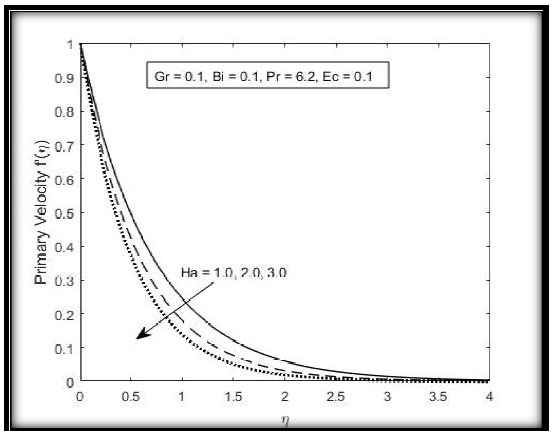

Fig. 5. Primary velocity profiles with increasing Ha

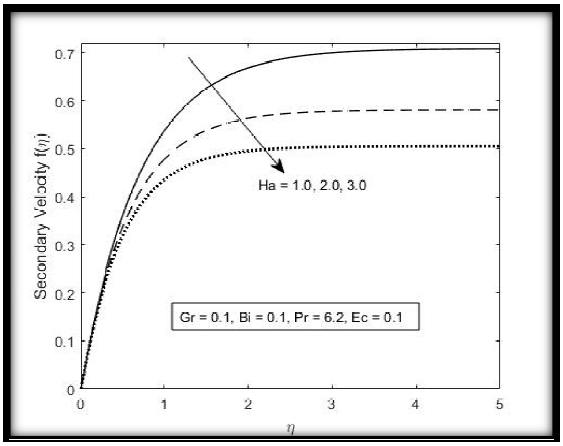

Fig. 6. Secondary velocity profiles with increasing Ha

Fig. 10 shows temperature profiles of the (Cu-Al_2O_3)/EG hybrid nanocoolant with increasing values of Ha i.e. $(Ha = 1.0, 2.0, 3.0)$. From the figure the temperature of the fluid increases with increasing values of Ha. The presence of the magnetic field results in joule heating in the fluid which is attributed to the increased friction force between the layers of the fluid resulting in the generation of heat energy that increases the temperature and the thickness of the thermal boundary layer of the fluid.

The Figs 11 and 12 show the effect of increasing Grashof number (Gr)on Primary and secondary velocity profiles of the hybrid nanocoolant. From the figures both the primary and secondary velocity profiles of the nanocoolant increases with increasing values of Grashof number (Gr)In Fig. 11 the velocity of the fluid is maximum on the surface of the moving plate and decays to zero value far away from the plate satisfying the given free stream condition.

The Figs. $(13 - 16)$ depicts the effect of Prandtl number (Pr) on primary and secondary velocity profiles of (Cu-Al_2O_3)/EG hybrid nanocoolant. From the figures the effect of Prandtl number (Pr) on the velocity profiles of the nanocoolant is negligible but in both cases, velocity profiles decrease with increasing Prandtl number (Pr).

The Figs. 17 and 18, shows how nanoparticle volume fraction and Grashof number (Gr) affects the temperature profile of the (Cu-Al_2O_3)/EG hybrid nanocoolant. Fig. 17 is plotted for increasing values of nanoparticle volume fraction $(\phi = 0.01, 0.1, 0.2)$ and figure 18 is plotted for increasing values of Grashof number $(Gr = 0.1, 2.0, 4.0)$. The results show that the temperature profile of the nanocoolant increases with increasing nanoparticle volume fraction and decreases towards the plate with increasing values of Grashof number (Gr) .

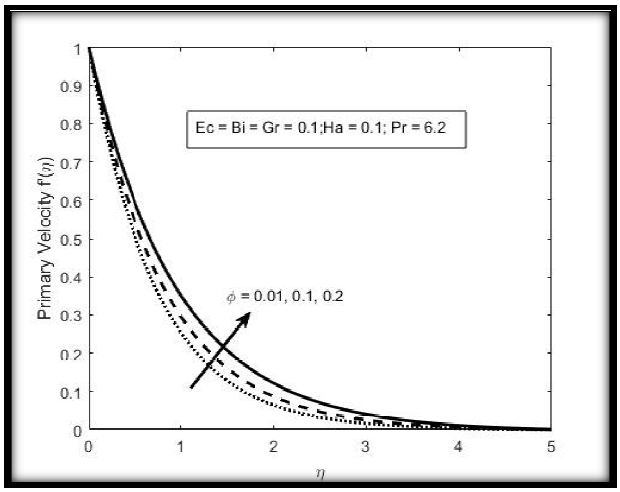

Fig. 7. Primary velocity profiles with increasing ϕ

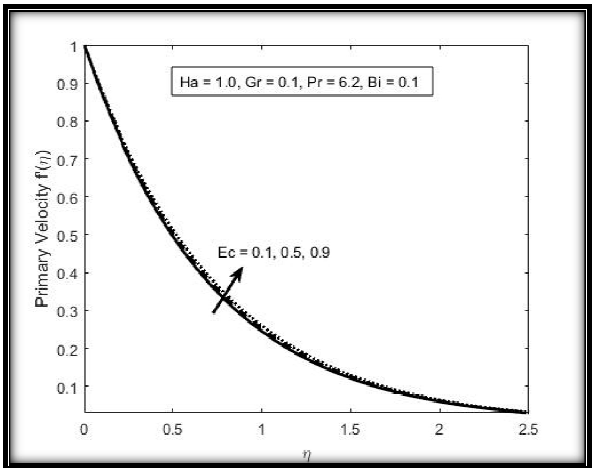

Fig. 8. Primary velocity profiles with increasing Ec

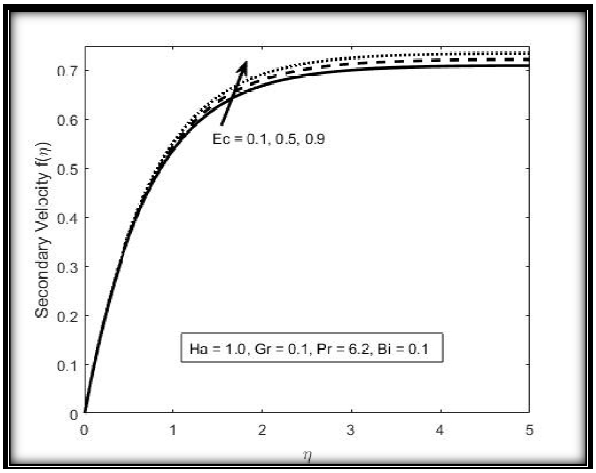

Fig. 9. Secondary velocity profiles with increasing Ec

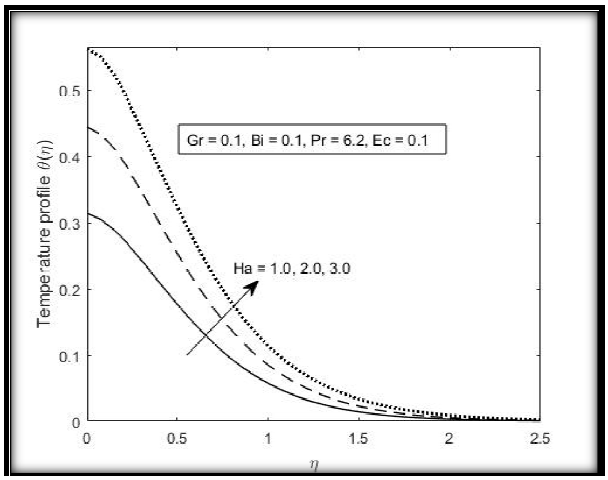

Fig. 10 Temperature profiles with increasing Ha

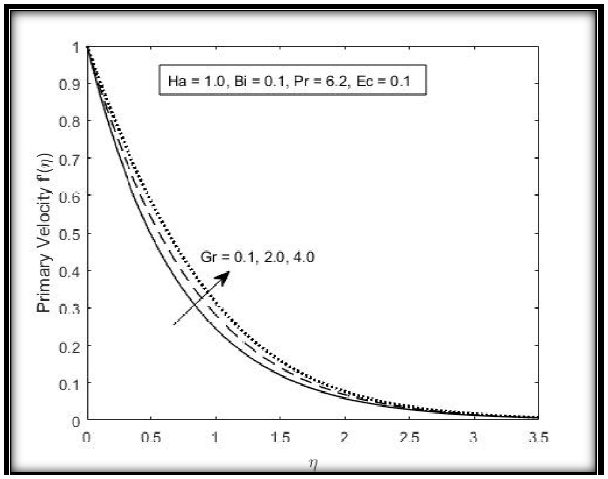

Fig. 11. Primary velocity profiles with increasing Gr

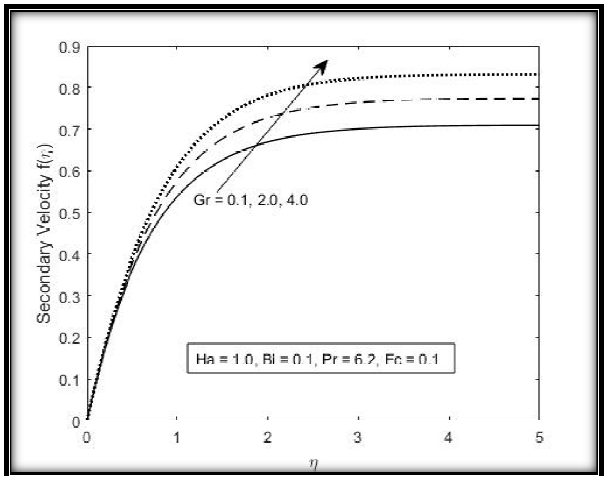

Fig. 12. Secondary velocity profiles with increasing Gr

For Figs. 19 and 20 the temperature profiles $\theta(\eta)$for the (Cu-Al_2O_3)/EG hybrid nanocoolant is plotted for increasing values of Biot number $(Bi = 0.1, 0.5, 0.9)$ and Eckert number $(Ec = 0.1, 0.5, 0.9)$ respectively. In both cases, the temperature profile increases with increasing values of Biot number and Eckert number.

Fig. 21 shows the temperature profiles $\theta(\eta)$ at different values of Prandtl number $(Pr = 2.0, 4.0, 6.20)$. From the figure, the temperature profile of (Cu-Al_2O_3)/ EG hybrid nanocoolant decreases with increasing values of the Prandtl number. The temperature is highest on the surface of the plate and decreases gradually to zero far away from the plate satisfying the given free stream condition.

3.3 Skin Friction Profiles and Nusselt Number Profiles of (Cu-Al_2O_3), (Cu-TiO_2) and (TiO_2-Al_2O_3) Ethylene-glycol Based Hybrid Nanocoolants

Figs. 22 and 23 shows Skin friction profiles and Nusselt number profiles (rate of heat transfer) of (Cu-Al_2O_3) /EG , (Cu-TiO_2) /EG, and (TiO_2-Al_2O_3)/EG hybrid Nanocoolants at the surface of the plate. The skin friction coefficient and the local Nusselt number is greatest in (Cu-Al_2O_3)/ EG hybrid nanocoolant compared to (Cu-TiO_2) /EG and (TiO_2-Al_2O_3) /EGhybrid Nanocoolants. The skin friction coefficient and the local Nusselt number decreases with increasing nanoparticle volume fraction in both hybrid nanocoolants as indicated in Figs. 22 and 23.

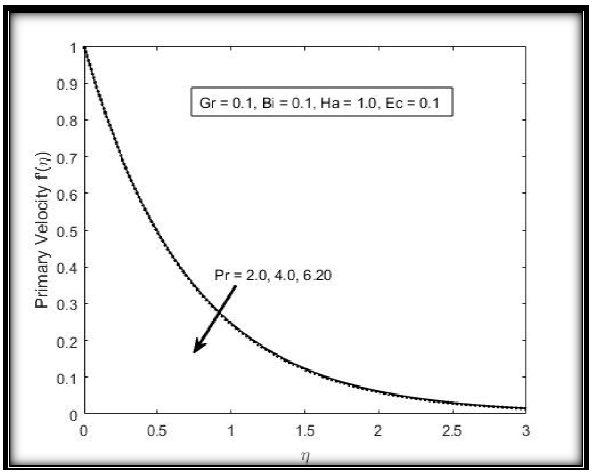

Fig. 13. Primary velocity profiles with increasing Pr

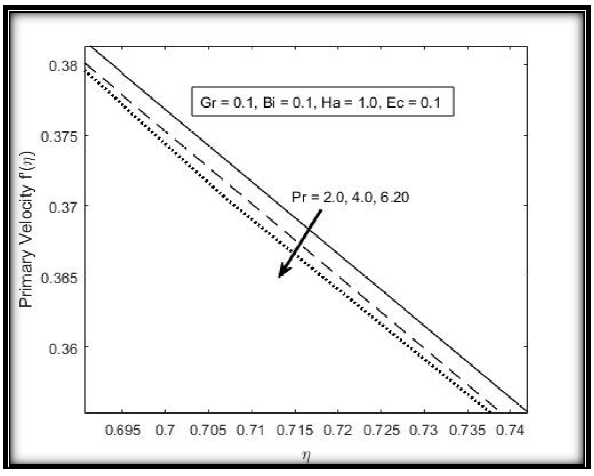

Fig. 14. Zoomed Primary velocity profiles with increasing Pr

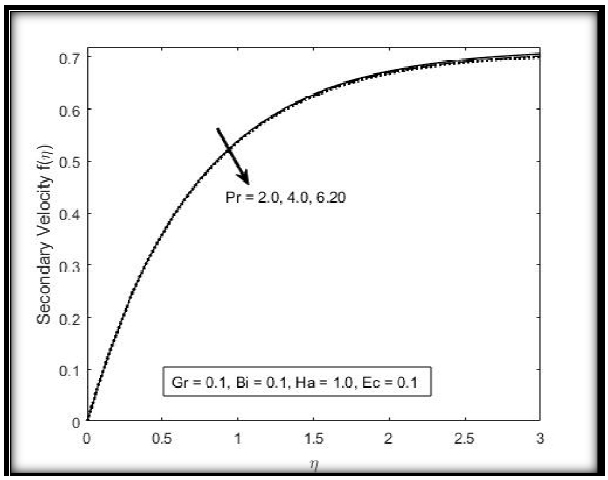

Figure 15: Secondary velocity profiles with increasing Pr

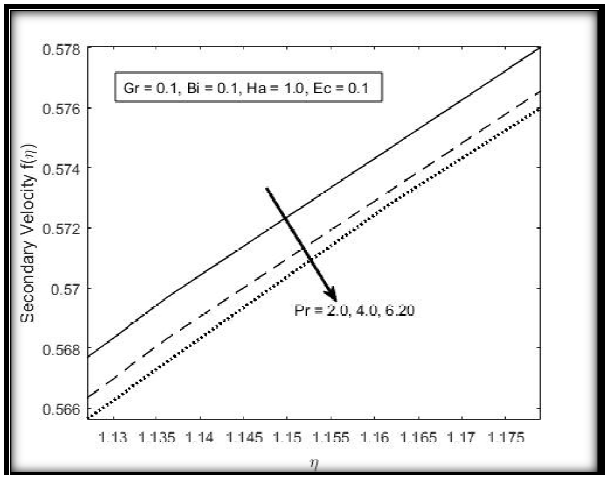

Fig. 16. Zoomed secondary velocity profiles with increasing Pr

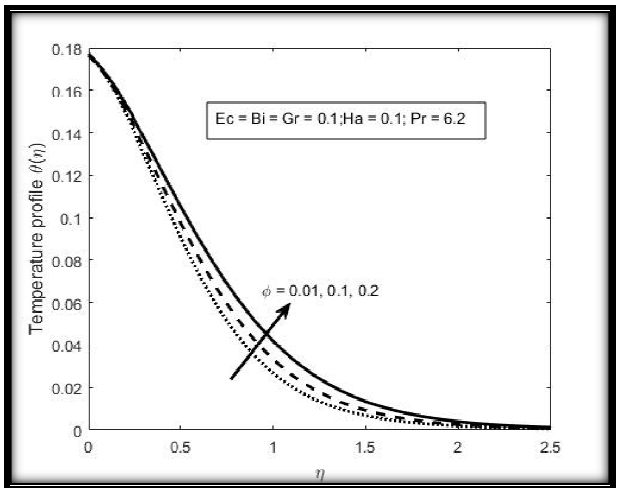

Fig. 17. Temperature profiles with increasing ϕ

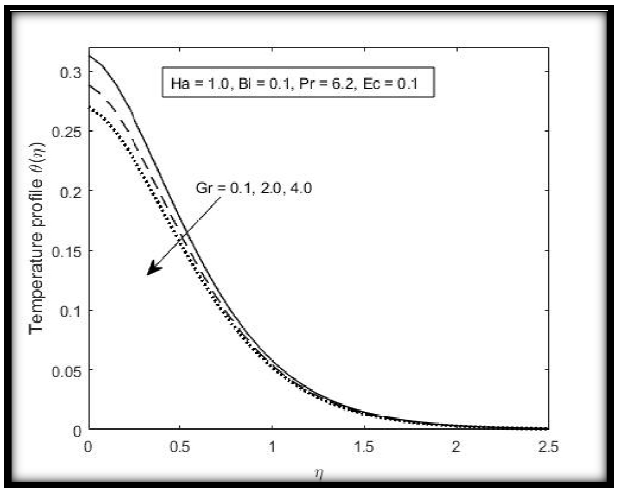

Fig. 18. Temperature profiles with increasing Gr

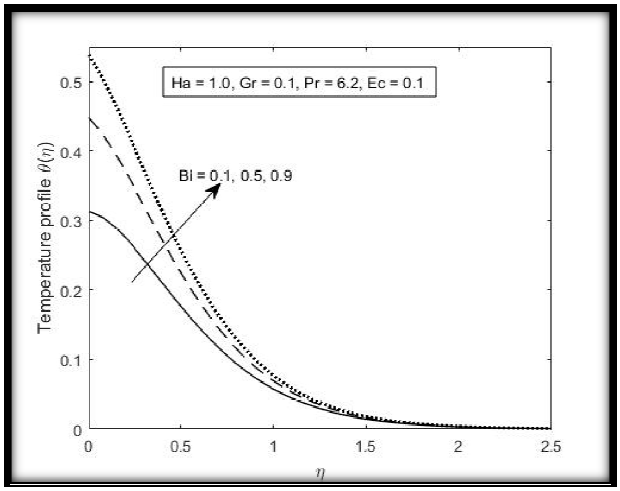

Fig. 19. Temperature profiles with increasing Bi

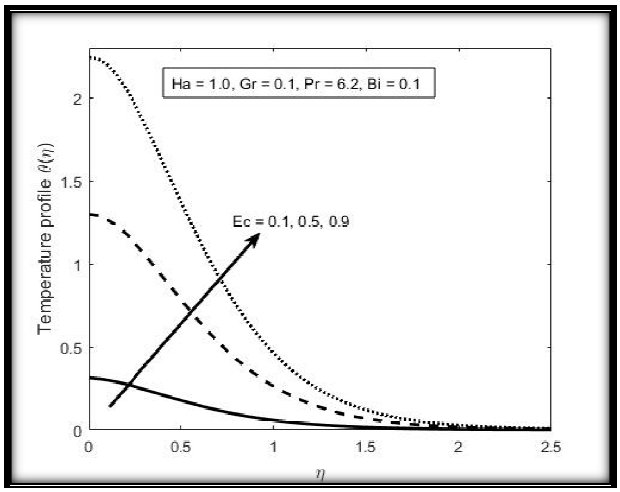

Fig. 20. Temperature profiles with increasing Ec

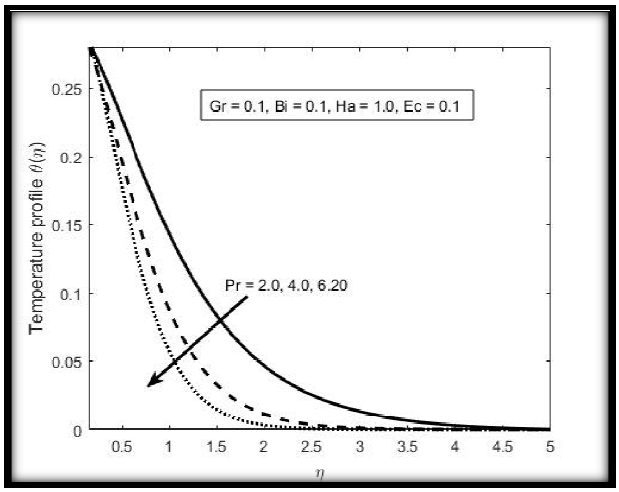

Fig. 21. Temperature profiles with increasing Pr

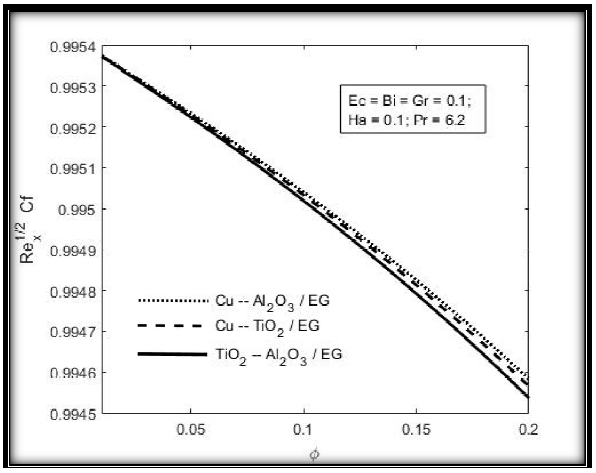

Fig. 22. Skin friction profiles for different hybrid nanocoolants

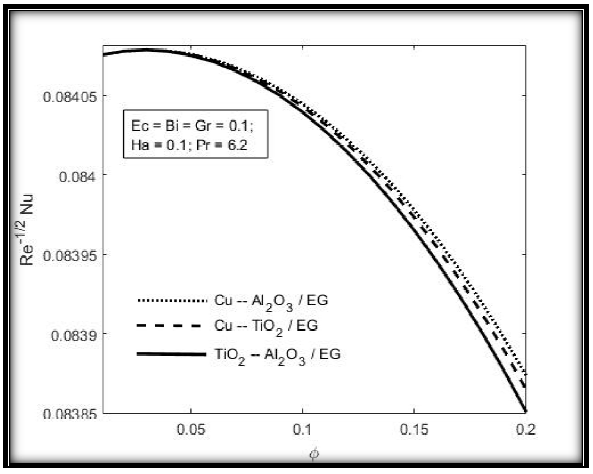

Fig. 23. Nusselt number for different hybrid nanocoolants

Table 1. Thermophysical properties of Ethylene-glycol and nanoparticles

Property	EG	Cu	Al_2O_3	TiO_2
ρ	1114	8933	3970	4250
C_p	2415	385	765	686.2
k	0.252	401	40	8.9538
β	57×10^{-5}	1.67×10^{-5}	0.85×10^{-5}	0.9×10^{-5}
σ	5.5×10^{-6}	5.96×10^{7}	3.5×10^{7}	2.38×10^{6}

4. CONCLUSION

Three different ethylene-glycol based hybrid nanocoolants ((Cu-Al_2O_3), (Cu-TiO_2), (TiO_2-Al_2O_3)) have been investigated to determine the suitable coolant candidate for use in the car radiator. The governing non-linear partial differential equations of fluid flow were transformed into a system of coupled non-linear ordinary differential equations using a suitable similarity transformation variables and the numerical solution was executed using the shooting technique together with the fourth-order Runge-Kutta-Fehlberg integration scheme. The numerical simulation was performed using MATLAB and the results displayed graphically. The effects of pertinent parameters on velocity, temperature, skin friction, and local Nusselt number were investigated. The conclusions drawn from the study are stated as follows:

i. The velocity of the fluid decreases with increasing values of magnetic field strength (Ha) and Prandtl number (Pr) and increases with increasing Eckert number (Ec), nanoparticle volume fraction (ϕ) and Grashof number (Gr).
ii. The temperature of the fluid increases with increasing values of magnetic field strength (Ha), Biot number (Bi), Eckert number (Ec), nanoparticle volume fraction (ϕ) and decreases with increasing values of Grashof number (Gr) and Prandtl number (Pr).
iii. The (Cu-Al_2O_3) $/EG$ hybrid nanocoolant exhibits a faster heat transfer rate compared to (Cu-TiO_2) $/EG$ and (TiO_2-Al_2O_3)$/EG$ hybrid nanocoolants.
iv. For all the three hybrid nanocoolants the skin friction coefficient and Nusselt number decreases with increasing nanoparticle volume fraction (ϕ).

From the application point of view, the cooling effect on the plate surface is maximized by enhancing the rate of heat transfer at the plate surface. From the results obtained this is achieved by employing (Cu-Al_2O_3 / EG) hybrid nanofluid as a coolant under the influence of magnetic field.

COMPETING INTERESTS

Authors have declared that no competing interests exist.

REFERENCES

1. Choi SUS. Enhancing thermal conductivity of fluids with nanoparticles. American Society of Mechanical Engineers, Fluids Engineering Division (Publication) FED; 1995.
2. Abbas F, Ali HM, Shah TR, Babar H, Janjua MM, Sajjad U, Amer M. Nanofluid: Potential evaluation in automotive radiator. Journal of Molecular Liquids. 2020;297(xxxx). Available:https://doi.org/10.1016/j.molliq.2019.112014
3. Yan S-R, Toghraie D, Abdulkareem LA, Alizadeh A, Barnoon P, Afrand M. The rheological behavior of MWCNTs–ZnO/Water–Ethylene glycol hybrid non-Newtonian nanofluid by using of an experimental investigation. Journal of Materials Research and Technology, 2020;9(4):8401–8406.
4. Boroomandpour A, Toghraie D, Hashemian M. A comprehensive experimental investigation of thermal conductivity of a ternary hybrid nanofluid containing MWCNTs- titania-zinc oxide/water-ethylene glycol (80:20) as well as binary and mono nanofluids. Synthetic Metals. 2020;268:116501.
5. Madhesh D, Parameshwaran R, Kalaiselvam S. Experimental investigation on convective heat transfer and rheological characteristics of Cu–TiO2 hybrid nanofluids. Experimental Thermal and Fluid Science. 2014;52:104–115.
6. Mosayebidorcheh S, Sheikholeslami M, Hatami M, Ganji DD. Analysis of turbulent MHD Couette nanofluid flow and heat

transfer using hybrid DTM–FDM. Particuology. 2016;26:95–101.
7. Hassan M, Ellahi R, Zeeshan A, Bhatti MM. Analysis of natural convective flow of non-Newtonian fluid under the effects of nanoparticles of different materials: Journal of Process Mechanical Engineering. 2018;233(3):643–652.
8. Tayebi T, Chamkha AJ. Free convection enhancement in an annulus between horizontal confocal elliptical cylinders using hybrid nanofluids. Numerical Heat Transfer,Part A. 2016;70(10):1141–1156.
9. Soltani F, Toghraie D, Karimipour A. Experimental measurements of thermal conductivity of engine oil-based hybrid and mono nanofluids with tungsten oxide (WO3) and MWCNTs inclusions. Powder Technology. 2020;371:37–44.
10. Alrashed AAAA, Akbari OA, Heydari A, Toghraie D, Zarringhalam M, Shabani GAS, Seifi AR, Goodarzi M. (2018). The numerical modeling of water/FMWCNT nanofluid flow and heat transfer in a backward-facing contracting channel. Physica B: Condensed Matter, 2018;537:176–183.
11. Nagarajan FC, Kannaiyan S, Boobalan C. Intensification of heat transfer rate using alumina-silica nanocoolant. International Journal of Heat and Mass Transfer. 2020;149:119127.
12. Selvaraj V, Krishnan H. Synthesis of graphene encased alumina and its application as nanofluid for cooling of heat-generating electronic devices. Powder Technology. 2020;363:665–675.
13. Deriszadeh A, Monte F de. On Heat Transfer Performance of Cooling Systems Using Nanofluid for Electric Motor Applications. Entropy. 2020;22(99):22(1)99.
14. Pourrajab R, Noghrehabadi A, Hajidavalloo E, Behbahani M. Investigation of thermal conductivity of a new hybrid nanofluids based on mesoporous silica modified with copper nanoparticles: Synthesis, characterization and experimental study. Journal of Molecular Liquids. 2020;300:112337.
15. Mukherjee S, Chakrabarty S, Mishra PC, Chaudhuri P. Transient heat transfer characteristics and process intensification with Al2O3-water and TiO2-water nanofluids: An experimental investigation. Chemical Engineering and Processing - Process Intensification. 2020;150:107887.
16. Kumar PCM, Chandrasekar M. Heat transfer and friction factor analysis of MWCNT nanofluids in double helically coiled tube heat exchanger. Journal of Thermal Analysis and Calorimetry. 2020;2020:1–13.
17. Pourrajab R, Noghrehabadi A, Behbahani M, Hajidavalloo E. An efficient enhancement in thermal conductivity of water-based hybrid nanofluid containing MWCNTs-COOH and Ag nanoparticles: experimental study. Journal of Thermal Analysis and Calorimetry. 2020;2020:1–13.
18. Leong KY, Saidur R, Kazi SN, Mamun AH. Performance investigation of an automotive car radiator operated with nanofluid-based coolants (nanofluid as a coolant in a radiator). Applied Thermal Engineering. 2010;30(17–18):2685–2692.
19. Singh D, Toutbort J, Chen G. Heavy vehicle systems optimization merit review and peer evaluation; 2006.
20. M'hamed B, Che Sidik NA, Akhbar MFA, Mamat R, Najafi G. Experimental study on thermal performance of MWCNT nanocoolant in Perodua Kelisa 1000cc radiator system. International Communications in Heat and Mass Transfer. 206;76:156–161.
21. Mutuku WN. Ethylene glycol (EG)-based nanofluids as a coolant for automotive radiator. Asia Pacific Journal on Computational Engineering. 201;3(1):1.
22. Huminic G, Huminic A. Numerical analysis of hybrid nanofluids as coolants for automotive applications. International Journal of Heat and Technology. 2017';35(1):S288–S292.
23. Barzegarian R, Aloueyan A, Yousefi T. Thermal performance augmentation using water based Al 2 O 3 -gamma nanofluid in a horizontal shell and tube heat exchanger under forced circulation. International Communications in Heat and Mass Transfer. 2017;86:52–59.
24. Hussein AM. Thermal performance and thermal properties of hybrid nanofluid laminar flow in a double pipe heat exchanger. Experimental Thermal and Fluid Science. 2017;88:37–45.
25. Raei B, Shahraki F, Jamialahmadi M, Peyghambarzadeh SM. Experimental study on the heat transfer and flow properties of γ-Al2O3/water nanofluid in a double-tube heat exchanger. Journal of Thermal Analysis and Calorimetry. 2017;127(3):2561–2575.

26. Hung Y-H, Wang,W-P, Hsu Y-C, Teng T-P. Performance evaluation of an air-cooled heat exchange system for hybrid nanofluids. Experimental Thermal and Fluid Science. 2017;C(81):43–55.

27. Mutuku-Njane WN, Makinde OD. MHD Nanofluid flow over a permeable vertical plate with convective heating. Journal of Computational and Theoretical Nanoscience. 2014;11(3):667–675.

Peer-review history:
The peer review history for this paper can be accessed here:
http://www.sdiarticle4.com/review-history/61548